Journal of Radioanalytical and Nuclear Chemistry (2019) 319:327–337
https://doi.org/10.1007/s10967-018-6356-5

Selective uranium adsorption using modified acrylamide resins

Sameh H. Negm[1] · Abd Allh M. Abd El-Hamid[2] · Mohamed A. Gado[1] · Hassan S. El-Gendy[1]

Received: 15 September 2018 / Published online: 4 December 2018

Abstract
Polymeric matrices composed of *N*,*N*′-Methylenebis(acrylamide)/glycidyl methacrylate was prepared and modified producing two resins (GMA/MBA/OH and GMA/MBA/SO_3H). The adsorption of U(VI) ions onto the modified acrylamide resins was studied from synthetic and granite samples. For better understanding around the uranium mineralization and the rock-forming minerals of the hosted granitic rocks, to facilitate the choice of the appropriate ore-processing techniques, it was necessary to identify the mineral composition and the radiometric specifications of the used granitic rock. The synthesized adsorbents revealed a promising selective adsorption toward the U(VI) ions from its bearing solutions even with the competence of other cations.

Keywords Uranium · Acrylamide · Glycidyl methacrylate · Adsorption

Introduction

Uranium is considered one of the most serious pollutants when it enters the environment due to its radioactivity and poisoning characteristics. On the other hand, uranium is used in nuclear power production; therefore, the recovery of uranium from various primary and/or secondary resources (e.g. granitic rock, ores, and seawater) have received attention over the last few decades [1–6].

There are a large number strategies utilized for the recuperation of various metal ions, which include membrane separation, ion exchange, solvent extraction and adsorption techniques [5–10]; however, the adsorption on ion exchange material has become a more popular technique. Adsorption has been observed to be a predominant technique for the removal of various metal ions from aqueous media (water, wastewater, etc.). The adsorbents can be broadly classified into inorganic and organic based adsorbents, however, organically based adsorbents are more popular. Adsorption techniques afford a broader range of application than solvent extraction due to the large choice of solid adsorbent. The mechanisms of retention of metal ions by adsorption depend on the nature of the adsorbent and may include simple adsorption, chelation or ion exchange. Ion exchangers have the advantage of having good porosity and selectivity, which allows ion exchange materials to be used within the nuclear field to recover uranium from its bearing solutions in a high-purified form. A broad spectrum of resin types has been used for this purpose [11–20].

Glycidyl methacrylate (GMA) is an ester of methacrylic acid and a common monomer used in the creation of epoxy resins. GMA monomer has dual functionality, containing both methacrylic and epoxy groups, both of these groups readily react with a wide range of monomers and functionalized molecules to provide the user with maximum freedom and flexibility in polymer design. The dual functionality of GMA brings together the desirable properties of both methacrylic and epoxies, hence, GMA based adsorbents are receiving great attention. Glycidyl methacrylate has been used in a variety of applications including chromatographic separation, ion–resin exchange, catalysis, enzyme and adsorbents [2–4, 21, 22].

In this work, hydroxy and sulfonated glycidyl methacrylate (GMA)/*N*,*N*′-Methylenebis(acrylamide) (MBA) resins (GMA/MBA/OH and GMA/MBA/SO_3H) were synthesized and batch experiments were carried out in order to examine the adsorption characteristics of uranium on the

✉ Sameh H. Negm
samehnegm.nma@gmail.com

[1] Research Sector, Nuclear Materials Authority, 1681 Maadi-Kattameya Road, El Maadi, P.O. Box 530, Cairo, Egypt

[2] Production Sector, Nuclear Materials Authority, 1681 Maadi-Kattameya Road, El Maadi, P.O. Box 530, Cairo, Egypt

resins. The resulting adsorption conditions were applied to the recovery of uranium from Gattar granite leach liquor.

Experimental

Chemicals

Glycidyl methacrylate (GMA), 2,2′-Azobis(2-methylpropionitrile) (AIBN), and *N*,*N*′-Methylenebis(acrylamide) (MBA) were Aldrich Products, uranium nitrate was Merck product while the other used chemicals were Prolab products. All the chemicals are of the analar grade.

Synthesis of the hydroxy and sulfonate glycidyl methacrylate/acrylamide resins

Firstly, GMA/MBA copolymers beads containing 20 mol% of MBA were prepared by mixing 0.2 mol of MBA (cross-linker) with 0.8 mol of GMA (monomer) with stirring for 15 min, then the AIBN (initiator, 0.5%) was added and the mixture was stirred for other 15 min. till complete dissolution followed by adding 2-ethyl-1-hexanol (diluent). The resulted solution (continuous phase) was added dropwise to the discontinuous phase comprised of 2% polyvinyl alcohol solution (stabilizer, 2%) at 60 °C then was refluxed at 80 °C. After 8 h, the beads formed were left to be cooled at room temperature, decanted and washed with water and ethanol and finally dried.

The GMA/MBA/OH-resin was prepared by adding 50 mL of 0.1 M sulfuric acid to 10 g of GMA/MBA then a reflux condenser was attached to the system and the reaction mixture was stirred occasionally and heated on a water bath at 75 °C for 5 h. The formed hydrolyzed polymer was filtered, washed with water and ethanol and finally dried.

The GMA/MBA/SO_3H-resin was prepared by adding 10 g of GMA/MBA to a solution composed of 30 g sodium sulfite dissolved in isopropyl alcohol/water (60/225 mL), then the mixture was refluxed at 80 °C. The formed resin was filtered, washed with water and with ethanol and finally dried. GMA/MBA/SO_3H and GMA/MBA/OH were characterized by Fourier Transform Infrared Spectroscopy (Thermo Scientific, Nicolet iS10 FTIR Spectrometer).

The batch experiments

Effect of pH on U(VI) adsorption

The pH effect on U(VI) ions adsorption was investigated at the range of 1–6 (pH was adjusted using diluted NaOH and HNO_3 solutions) using a series of Erlenmeyer flasks, in each 0.02 g resin and 40 ml of U(VI) solution of initial concentration of 50 mg L^{-1} were allowed to react under shaking for 3 h (THERMOLAB® shaking water bath, model-1083, GFL Gesellschaft für Labortechnik mbH, Germany) at 25 °C. After equilibration, the residual concentration was measured using the UV/VIS spectrophotometer (LABOMED, INC, USA) according to the Arsenazo III method (measure the absorbance at 655 nm) [23]. The amount of adsorbed uranium ions as uptake (mg g^{-1}) or adsorption percentage (%) was calculated based on the following mass balance equations:

$$q\left(\mathrm{mgg}^{-1}\right) = \frac{\left(C_\mathrm{i} - C_\mathrm{e}\right)}{g} \times V$$

$$q(\%) = \frac{\left(C_\mathrm{i} - C_\mathrm{e}\right)}{C_\mathrm{i}} \times 100$$

where C_i (mg L^{-1}) is the initial concentration of U in the solution; C_e (mg L^{-1}) is the concentration of U in the filtrate; V(L) is the volume of initial solution; g(g) is the amount of adsorbent used.

Kinetics studies

The kinetics of the adsorption of U(VI) ions on GMA/MBA/OH and GMA/MBA/SO_3H were studied by placing and shaking 0.02 g of the adsorbents in U(VI) solution (40 mL; 120 mg L^{-1}; pH 5) for the required contact time (2–120 min) at 25 °C. The residual concentration was measured using the same method as described previously.

Effect of initial uranium concentrations and temperature on U(VI) adsorption

Effect of temperature on the adsorption process was studied in the range 25–500C and at different initial U(VI) ions concentrations (20–120 mg L^{-1}) using 40 mL U(VI) solution (pH 5). The flasks were shaken on a shaking water-bath model-1083 (GFL Gesellschaft für Labortechnik mbH, Germany) with microprocessor-controlled temperature regulation ensures fast heating up to the individually set temperature and an excellent temperature constancy: ±0.1 °C. After equilibration (contact time of 60 and 75 min for GMA/MBA/SO3H and GMA/MBA/OH, respectively), the residual concentration of metal ions was quantified to calculate the amount retained by resin.

Application on the uranium leach liquor of Gattar granite

Gattar granitic batholith locates between latitudes 26°52′ and 27°08′N and longitudes 33°13′ and 33°26′E at about 35 km to the west of Hurghada city, Egypt. Seven uranium occurrences were discovered in Gabal Gattar area by the

Nuclear Materials Authority and named serially as GI to GVII, the processed granite in this study was sampled from the GII occurrence [24, 25].

The mineralogical, autoradiographic and radiometric investigation

Four samples from GII area were subjected to the petrographic investigation to identify their main mineralogical constituents. The radiometric characteristics of Gattar granite have been defined by measuring thorium and uranium contents in eight randomly collected samples. Thorium and uranium contents were measured radiometrically using the laboratory γ-spectrometry technique (Multi-channel Gamma Spectrometer with NaI (Tl) detector). Also, uranium was measured chemically using the UV/Vis spectrophotometer [23]. The ratio of chemically measured uranium/radiometrically measured uranium (D-factor) was calculated and taken as guidance for uranium mobilization and the radiometric equilibrium in the investigated granite [26–28].

Chemical characterization of processed granite sample

Before it's subjected to the chemical analysis, the composite sample was crushed using the Jaw crusher then ground to less than 200 mesh in size by the ball mill. By careful quartering (to conduct complete homogeneity), a 0.5 g of the ground representative sample was properly digested till complete decomposition and finally obtained in a volume of 250 ml of double distilled water. The X-ray fluorescence technique, (XRF), was used to determine the element content within the studied samples using PHILIPS Unique-II spectrometer with automatic sample changer PW 1510, (30 positions). This instrument is connected to a computer system using X-40 program for spectrometry. The major and trace components were identified and estimated by the proper analytical techniques relevant to the measured elements [23, 29].

Recovery of uranium from leach liquor of Gattar granite

A composite representative granitic sample from Gattar area (occurrence II) was firstly crushed and ground to about − 200 mesh size and then uranium content was leached from it using sulfuric acid. The authors applied the optimum uranium leaching conditions from Gattar granite applied by Zahran et al. [24], with some modifications, under the leaching conditions of 1:4 (solid:liquid ratio), room temperature, 4 h (leaching time) and 10 kg ton^{-1} (sulfuric acid). The obtained leach liquor was chemically analyzed. 0.1 g of the studied sorbents was stirring in 25 ml of the leach liquor with different pHs for for 15 min. The equilibrium concentrations of the different constituents were determined and were used to evaluate the extraction percentage (adsorption (%)). The effect of time on uranium extraction was studied; 0.1 g of the adsorbents was stirring in 25 ml of granite leach liquor at pH 4 for different shaking time, where keeping other parameters constant.

Results and discussion

The hydrolysis of the epoxide groups of the poly (GMA/MBA) into vicinal diol groups takes place under catalysis with mineral acid. When the reaction was carried at room temperature the hydrolysis was not completed. The epoxide groups of the prepared resin were hydrolyzed when treated with dilute sulfuric acid at 80 °C (Fig. 1a), this was characterized by IR spectroscopy (Nicolet IS-10 FTIR spectrophotometer) to check the extent of hydrolysis. The IR spectrum pointed to the successful hydrolysis of the epoxide groups, hydroxylation of epoxide group into a diol when the reaction mixture was catalyzed by 0.1 M sulfuric acid (Fig. 1b).

Factors affecting the U(VI) adsorption

Effect of pH

Results of the solution pH effect on the uranium (VI) sorption onto GMA/MBA/SO_3H and GMA/MBA/OH (Fig. 2) show that uranium (VI) adsorption capacity increases with pH increasing from 2.0 to 5.0 for GMA/MBA/SO_3H and GMA/MBA/OH, and then the adsorption capacity remained constant after pH 5 for the both resins. At the low pH values (< 2), the predominate existed uranium(VI) species is the uranyl cations UO_2^{2+} which will be not favorable for adsorption due to the strong competition on the binding active sites of the adsorbents with the available high H^+ concentration. Also, effective adsorption will not occur at low pH due to repulsion between UO_2^{2+} and protonated adsorbent groups [20]. On the other hand, at greater pH values (2–6) uranium(VI) presents as uranyl cations UO_2^{2+}, while the protonation degree is considerably reduced hence, the former competition turns to the side of the uranium cations consequently their adsorption is intensified. The polynuclear hydroxo-uranyl cations as $(UO_2)_3(OH)_5^+$, $(UO_2)_2(OH)_2^{2+}$, $(UO_2)_4(OH)_7^+$, $(UO_2)_4(OH)_6^{2+}$, $(UO_2)_4(OH)_2^{6+}$ have a lower chance at being adsorbed [2–4, 30–33].

Effect of contact time and adsorption dynamics

Effect of the contact time was examined in the range of 2–120 min (Fig. 3a) at 25 ºC. Generally, the adsorption capacity of uranium by both resins increased with increasing of the contact time and the adsorption equilibrium was

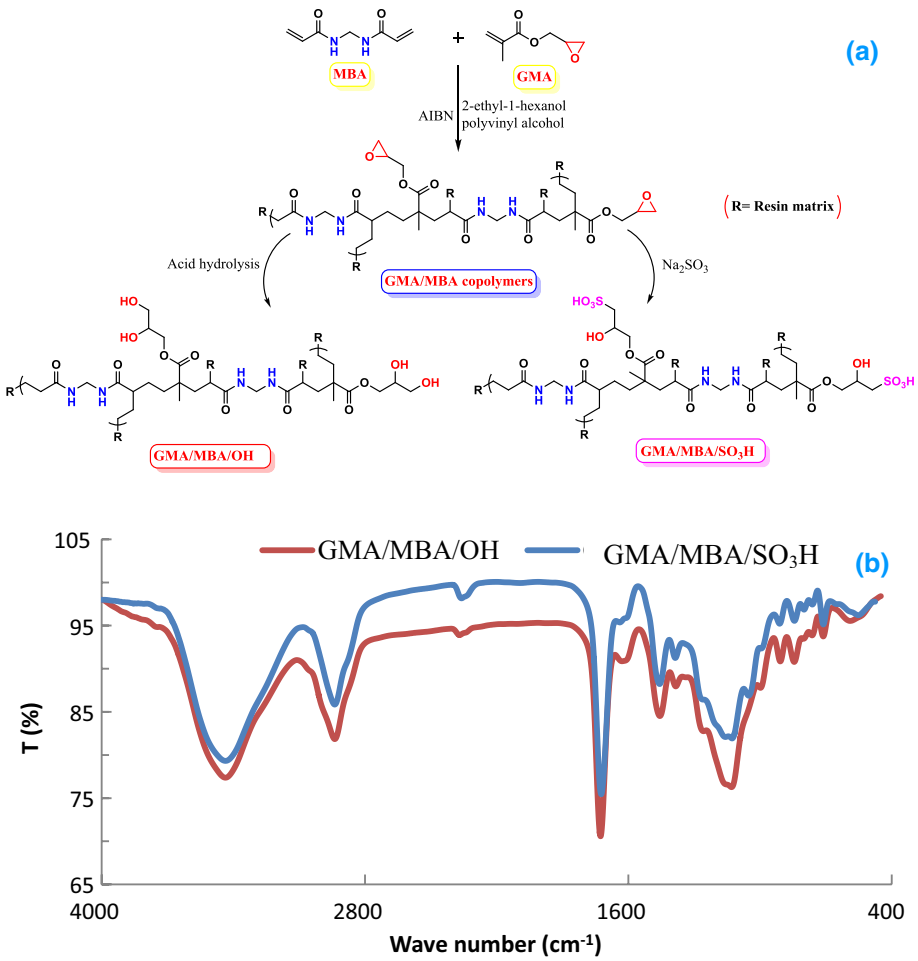

Fig. 1 Synthesis route (**a**), IR spectra (**b**) of GMA/MBA/OH and GMA/MBA/SO_3H

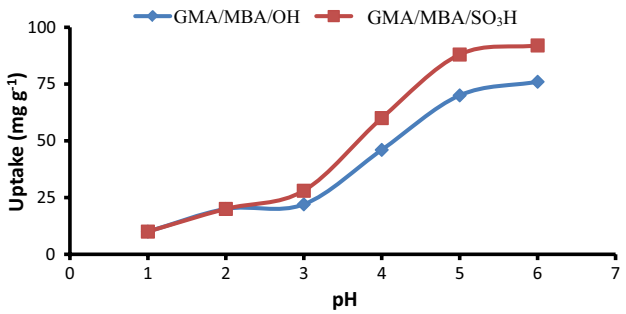

Fig. 2 Effect of initial pH on adsorption of uranium(VI) by GMA/MBA/OH and GMA/MBA/SO_3H

attained with 60 and 75 min with GMA/MBA/SO_3H and GMA/MBA/OH, respectively.

The data were treated with two kinetic models, the pseudo-first (Eq. 3) and pseudo-second-order models (Eq. 4), to evaluate kinetic parameters [33–35].

$$\log\left(q_e - q_t\right) = \log q_1 - \frac{k_1}{2.303}t \tag{3}$$

$$\frac{t}{q_t} = \frac{1}{k_2 q_2^2} + \left(\frac{1}{q_2}\right)t \tag{4}$$

where q_e is the amount of uranium sorbed on GMA/MBA/SO_3H and GMA/MBA/OH (mg g^{-1}) at equilibrium; q_t is the amount of uranium sorbed on GMA/MBA/SO_3H and GMA/MBA/OH (mg g^{-1}) at time t; k_1 is the rate constants for the pseudo-first-order model; k_2 is the rate constants for the pseudo-second-order; q_1 and q_2 are the theoretical capacity from the pseudo-first and pseudo-second-order models, respectively.

The kinetic parameters were assessed from the two models while the relating comes about were appeared in Table 1. Referring to values of the theoretical adsorption capacity and the experimental adsorption capacity as well as the corrosion coefficient (R^2) values in both models for the two used resins it is logically to said that the adsorption process by both the resins follows the pseudo-second-order model (Fig. 3b) and that the reaction rate depends on both adsorbent and adsorbate.

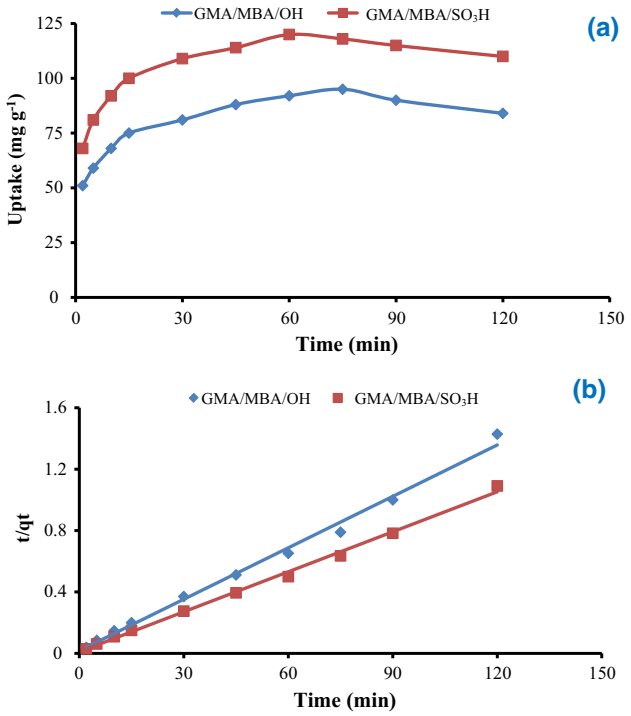

Fig. 3 Effect of contact time (**a**) and pseudo 2nd order kinetics plot for the adsorption of U(IV) onto GMA/MBA/OH and GMA/MBA/SO_3H (pH 5, 25 °C, 40 mL, 0.02 g adsorbent and 120 mg L^{-1} U(VI)

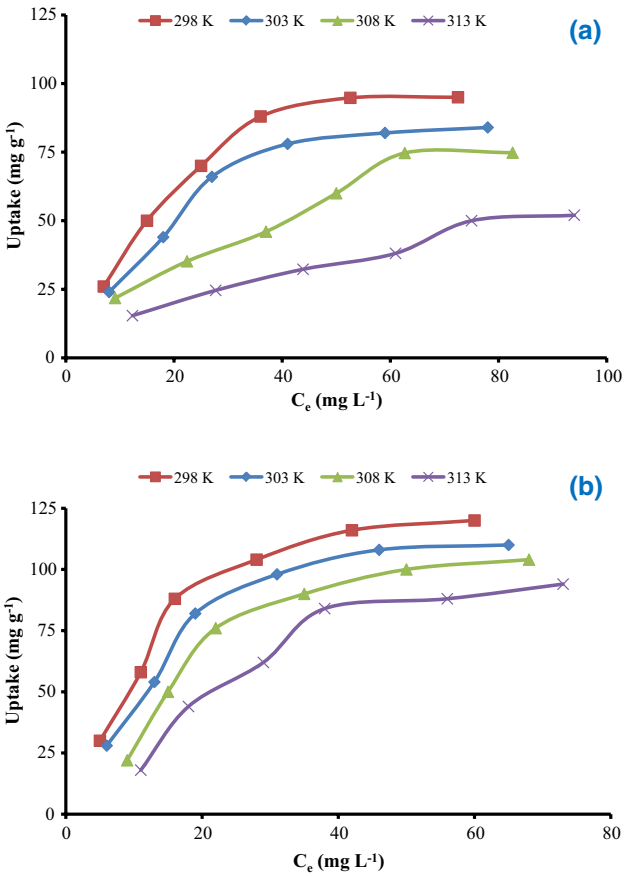

Fig. 4 Effect of initial uranium concentration on at different temperature on its loading by GMA/MBA/OH (**a**) and GMA/MBA/SO_3H (**b**)

Effect of initial uranium concentrations

Figure 4 shows the effect of the initial uranium concentration on its adsorption upon GMA/MBA/SO_3H and GMA/MBA/OH. The results revealed that with increasing the initial uranium concentration, the amount of uranium-loaded on the working adsorbents (mg g^{-1}) was increased. With the higher concentrations, the loaded uranium amounts approximately remained constant reflecting that the adsorbents reached their saturation capacities. The proportional increasing between the initial uranium concentration and the adsorption capacity is likely to be interpreted due to the high mobility of uranyl ions in the solutions that enhances the interactions of these ions with the adsorbents [2–4, 30–33].

Sorption isotherm

The sorption isotherm of the uranium adsorption by the prepared GMA/MBA/SO_3H and GMA/MBA/OH resins was investigated using different temperatures (25, 30, 35 and 40 °C) with employing the Freundlich and Langmuir isotherm models to analyze the uptake isotherms and the fitness of the obtained isotherm data.

Freundlich model refers to the multilayer sorption and for the sorption on heterogeneous surfaces [33–35]. The logarithmic form of Freundlich model is given by the equation:

$$\log q_e = \log K_f + \frac{1}{n} \log C_e \quad (5)$$

where K_f is the constant indicative of the relative adsorption capacity of the GMA/MBA/SO_3H and GMA/MBA/OH (mg g^{-1}), C_e the equilibrium concentration of the metal ion in the equilibrium solution (mg L^{-1}) and $1/n$ is the constant indicative of the intensity of the adsorption process.

Table 1 Pseudo-first and Pseudo-second order model parameters of U(VI) sorption onto GMA/MBA/SO3H and GMA/MBA/OH

Adsorbents	q_e	1st order kinetics			2nd order kinetics		
		k_1	q_1	R^2	k_2	q_2	R^2
GMA/MBA/OH	95	0.01543	25.527	0.4811	0.0072	89.286	0.9934
GMA/MBA/SO_3H	120	0.01819	27.574	0.5246	0.0075	120.482	0.9968

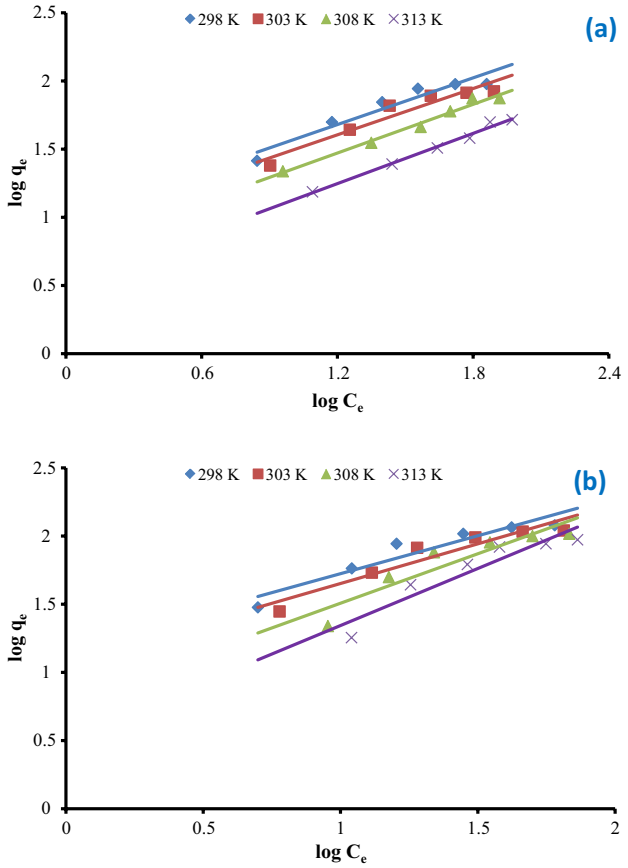

Fig. 5 Freundlich equilibrium isotherm model for the sorption of the U(VI) ions from aqueous solution using GMA/MBA/OH (**a**) and GMA/MBA/SO_3H (**b**)

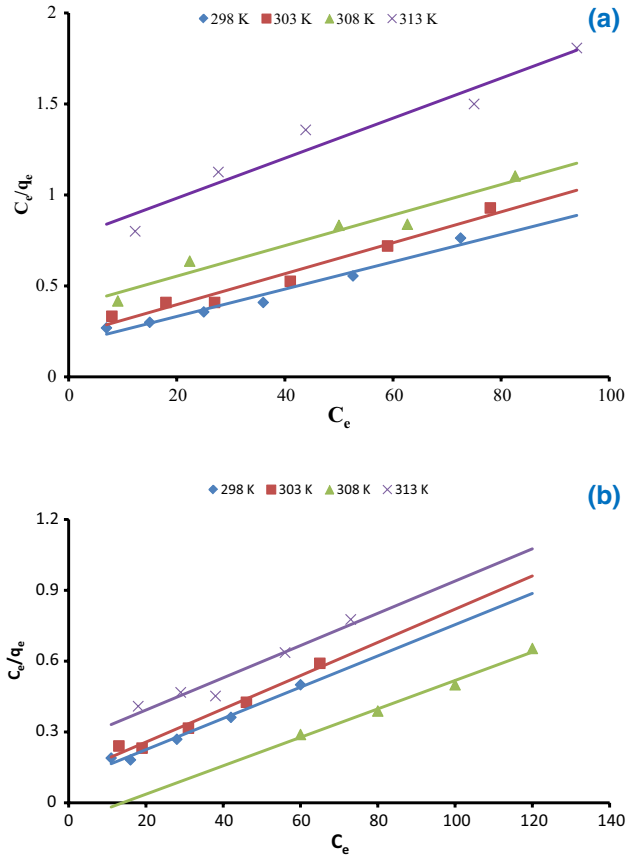

Fig. 6 Langmuir equilibrium isotherm model for adsorption of the U(VI) ions from aqueous solution using GMA/MBA/OH (**a**) and GMA/MBA/SO_3H (**b**)

The relation of Log q_e versus Log C_e for GMA/MBA/SO_3H and GMA/MBA/OH were drawn (Fig. 5a and b). The low R^2 coefficient value and the large difference between the calculated and experimental values of adsorption capacity indicate that the sorption mechanism of uranium (VI) on GMA/MBA/SO_3H and GMA/MBA/OH doesn't obey Freundlich equilibrium isotherm (Table 2).

Langmuir model refers to the monolayer sorption system on homogeneous surfaces [36–38]. The logarithmic type of Langmuir system is given by Eq. 6.

$$\frac{C_e}{q_e} = \frac{C_e}{Q_m} + \frac{1}{K_L Q_m} \tag{6}$$

where q_m (mg g^{-1}) is the maximum capacity, and K_L (L mg^{-1}) is the adsorption equilibrium constant. Plotting of

Table 2 Langmuir and Freundlich equilibrium constants for U(VI) ions by GMA/MBA/SO_3H in aqueous solution

Adsorbents	T	Langmuir isotherm				Freundlich isotherm		
		K_L	Q_m	R^2	q_e	K_f	$1/n$	R^2
GMA/MBA/OH	298	0.041	133.33	0.9707	95	9.89	0.57	0.9280
	303	0.037	117.65	0.9668	84	8.42	0.57	0.9193
	308	0.022	119.05	0.9520	74.8	5.71	0.60	0.9824
	313	0.014	90.91	0.9422	52	3.237	0.61	0.9889
GMA/MBA/SO_3H	298	0.027	147.06	0.9413	120	14.73	0.56	0.9037
	303	0.060	142.86	0.9751	110	11.75	0.59	0.9047
	308	0.071	151.52	0.9842	100	6.05	0.72	0.8519
	313	0.072	166.67	0.9892	94	3.21	0.84	0.8830

C_e/q_e versus C_e for GMA/MBA/SO_3H and GMA/MBA/OH (Figs. 6a and b) resulted in a straight line with a slope of $[1/Q_m]$ and an intercept of $[1/(Q_m K_L)]$ show that the adsorption process obeys Langmuir adsorption model. The parameters of R^2, Q_m and K_L (Table 2) indicate that both the GMA/MBA/SO_3H and GMA/MBA/OH show a better adsorption capacity at 298 K and fit satisfy to Langmuir equilibrium model.

Application on the uranium leach liquor of Gattar granite

For better understanding around the uranium mineralization and the rock-forming minerals of the hosted granitic rocks to facilitate choosing of the appropriate ore-processing techniques, it was necessary to identify the mineral composition, particularly the accessory and radioactive minerals, and the radiometric specifications of the used granitic rock.

The mineralogical, autoradiographic and radiometric investigation

Four samples from GII area were subjected to the petrographic investigation which pointed to that the main mineralogical constituents are represented in quartz, perthite, plagioclase and comparable amounts of biotite and muscovite (Figs. 7a–d). The accessory minerals were recognized as zircon, sphene, fluorite, and opaques (Figs. 7c–f). Some of the opaque minerals are highly expected to be primary radioactive minerals as has been seemed from the autoradiograph investigation. Secondary minerals were identified as saussurite, sericite, chlorite and iron oxides as alteration products of the plagioclase, perthite, muscovite and biotite respectively [24, 25, 39, 40].

Hosting of uranium into the accessory minerals, especially zircon, is clearly verified through the pleochroic halos appeared in the major minerals that enclose zircon or adjacent to it, such halos are happened by the effect of the alpha bodies that emitted from the admitted uranium into the crystal structure of these accessory minerals (Fig. 7d). Also, the alpha tracks which appeared on the developed sensitive films

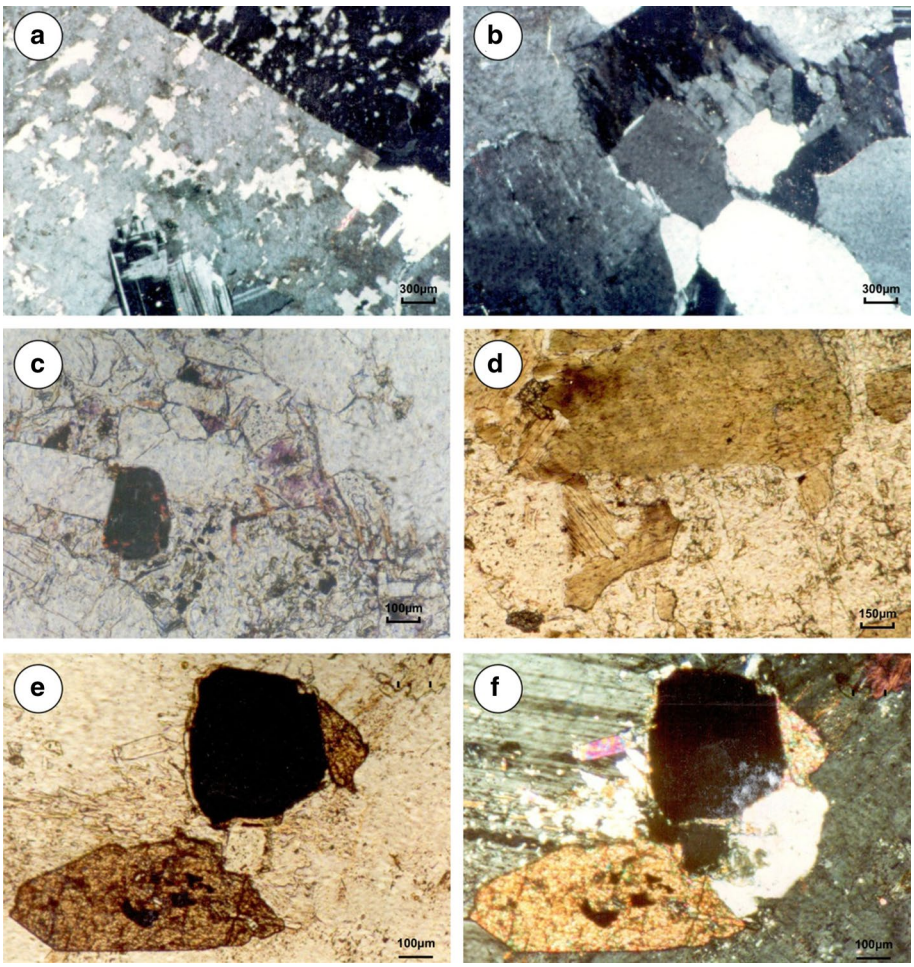

Fig. 7 **a** orthoclase perthite of patchy type enclosing plagioclase crystals under the polarized microscope (CP), **b** anhedral quartz crystals corrode into the orthoclase perthite under CP, **c** aggregation of violet fluorite crystals under the polarized lens (PL), **d** partially chloritized biotite flake under PL, **e** wedged sphene crystal with minute crystals of muscovite and fluorite as well as subhedral opaque mineral under PL, **f** same description of **e** under the CP

confirmed the hosting of the uranium inside the accessory minerals (Fig. 8a, b). On the other hand, the dense alpha tracks by some opaque minerals (Fig. 8c–f) strongly support them as primary uranium minerals (uraninite and/or pitchblende) particularly with the low thorium content as has been revealed later in this study [25, 39].

In this study, the secondary uranium minerals could not be recognized but many workers identified some of them such as; uranophane, beta-uranophane, and kasolite in Gattar granite [25, 26, 39, 40]. Generally, distribution of the uranium among the accessory minerals and the probable primary uranium minerals as well as the secondary uranium mineralization indicates the needing for careful processing and leaching conditions to conduct the maximum uranium leaching efficiency. For this goal, the leaching process shall consider the resistance of accessory minerals for leaching and decomposition under normal working conditions and that the primary uranium minerals contain the uranium in its immobilized form (U^{4+}).

The radiometric characteristics of Gattar granite have been defined by measuring thorium and uranium contents in eight randomly collected samples and the obtained data are illustrated in Table 3. *D*-factor value more or lesser than unity indicates the uranium mobilization by addition or removal respectively. The investigated samples revealed the presence of both assumptions that point to the role played by meteoric water and/or hydrothermal solutions as carriers for the transported uranium. Also, it gives a good potentiality for the presence of the hexa-valance uranium in considerable amounts which easily leached from the host granite.

The chemical characterization of the processed granitic sample

One composite granitic sample from the GII occurrence was carefully sampled taking into account its representation for the variable uranium concentrations in this occurrence to conduct a trusted estimation about the uranium leaching efficiency. The major and the trace constituents were estimated and the information was outlined in Table 4.

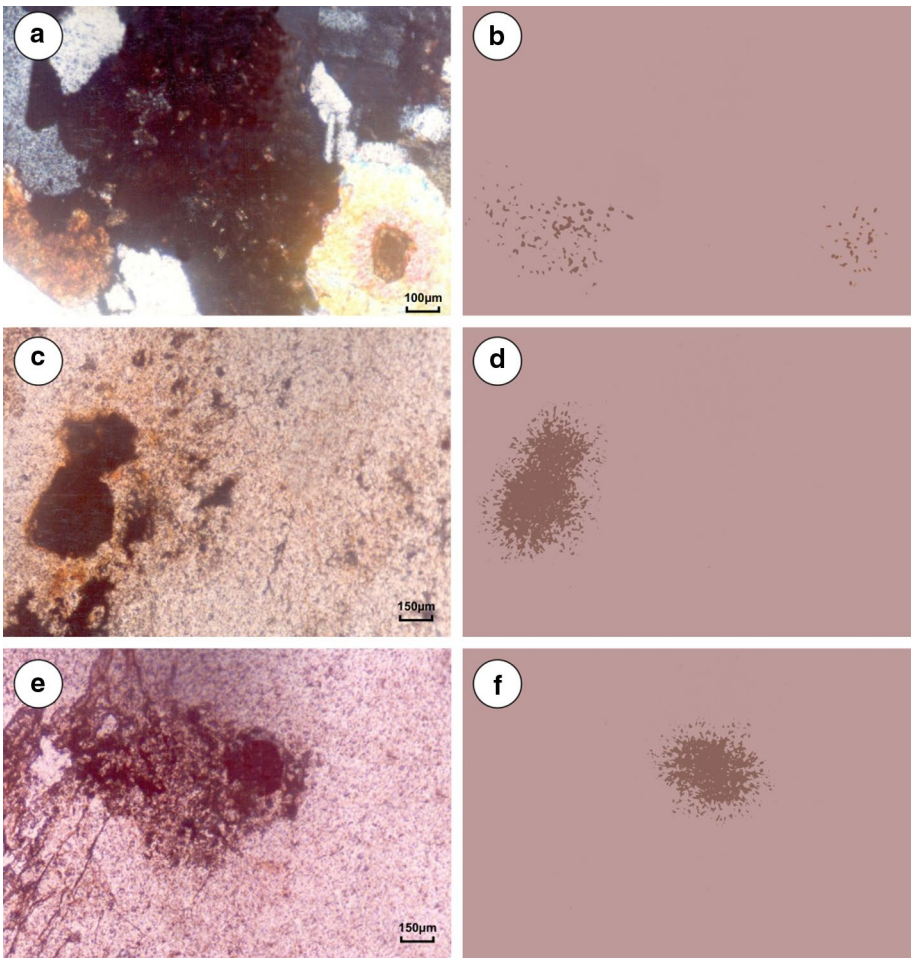

Fig. 8 **a**, **b** show partially metamicted zircon crystals and their α-trakes respectively, **c**–**f** show black radioactive minerals with their dense α-trakes respectively

Table 3 Th and U contents and D-factors of the investigated Gattar granitic samples (GII occurrence)

Sample	Th (ppm)	$U_{chem.}$ (ppm)	U_{rad} (ppm)	*D*-factor ($U_{chem.}$/$U_{rad.}$)
1	19	93	165	0.56
2	39	186	98	1.90
3	42	174	202	0.86
4	54	630	485	1.30
5	263	1666	1210	1.38
6	48	220	587	0.37
7	110	1200	1540	0.78
8	131	1280	924	1.39

Recovery of uranium from leach liquor of Gattar granite

A composite representative granitic sample from Gattar area (occurrence II) was subject to uranium leaching process and the obtained leach liquor was chemically analyzed (Table 5) where the determined uranium concentration (150 ppm) indicated that the uranium leaching efficiency reached to (95%). Iron and manganese are elements that affect uranium extraction from granite leach liquors. Accordingly, uranium, as well as iron and manganese extraction by the studied adsorbent was studied from the granite leach liquor. The equilibrium concentrations of the different constituents were determined and were used to evaluate the extraction percentage (adsorption (%)). The outcomes demonstrate that the extraction of uranium increases with increasing pH value. The maximum extraction efficiency of iron and manganese was in the range 29–30.6 and 19–46%, on GMA/MBA/OH and GMA/MBA/SO_3H, respectively. The studied sorbents show selective extraction of uranium (60%) at pH value of 4–5 (Fig. 9a, b). The results obtained from the effect of time on uranium extraction show selective extraction properties of uranium over manganese and iron at all the studied time (except 5 mint). It is was found that the adsorption capacity of uranium increases with increasing contact time and adsorption equilibrium was attended within 75 min (Fig. 10a, b). Extraction of uranium increases with time until it reaches a maximum value of 80 and 81.5% by GMA/MBA/OH and GMA/MBA/SO_3H, respectively. Elution of the adsorbed heavy metals was carried out using 0.1 M EDTA, where uranium was eluted using 0.01 M nitric acid.

Table 5 Chemical analysis of the granite leach liquors used in the extraction process

Metal Ion	Concentration (mg L^{-1})
U	150
Fe	1050
V	85
Mn	280
Ti	30

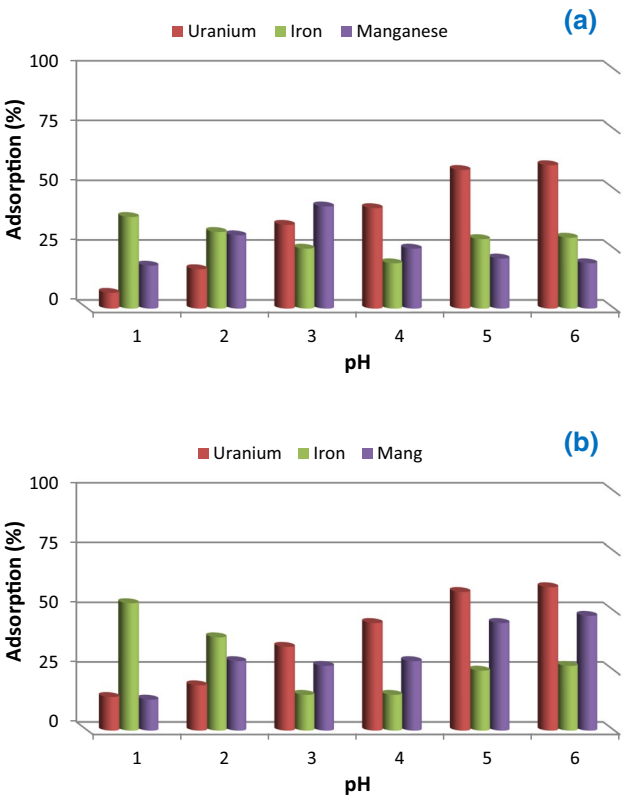

Fig. 9 Effect of pH on adsorption of uranium, iron and manganese from granite leach liquor by GMA/MBA/OH (**a**) and GMA/MBA/SO_3H (**b**)

Table 4 The chemical composition of the studied granitic composite sample

Major	SiO_2	TiO_2	Al_2O_3	Fe_2O_3	MnO	MgO	CaO	Na_2O	K_2O	P_2O_5	l.O.I
(%)	77.23	00.04	12.10	02.60	00.03	00.05	00.70	03.10	03.60	00.05	00.85
Trace (ppm)	Ga	U	Rb	Sr	Zr	Ba	Nb	Y	Zn		
	93	630	185	25	204	98	105	98	180		

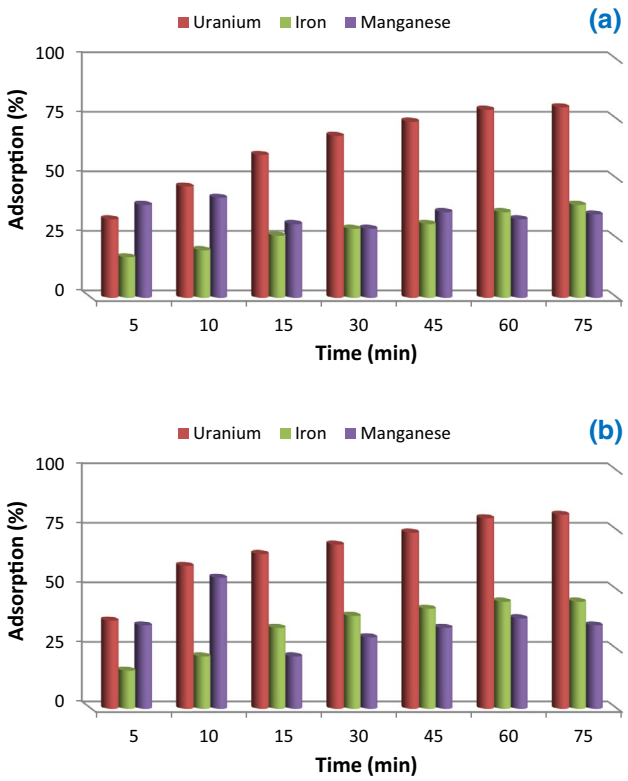

Fig. 10 Effect of time on adsorption of uranium, iron and manganese from granite leach liquor by GMA/MBA/OH (**a**) and GMA/MBA/SO_3H (**b**)

Conclusions

Based on the above-illustrated results and discussion some conclusions could be summarized in different points. The synthesized new adsorbents, GMA/MBA/SO_3H and GMA/MBA/OH, revealed a promising selective adsorption toward the U(VI) ions from its bearing solutions even with the competence of other cations. The exothermic nature of the adsorption process by GMA/MBA/OH and GMA/MBA/SO_3H adsorbents mirrors their practicality from the energy consumption point of view. The two adsorbents are recommended as promising candidates for high-efficient and selective removal and/or adsorption of uranium from the leach liquors of its bearing ores or from the contaminated aqueous solutions (radioactive liquid wastes). Finally, the two adsorbents are encouraged for further studies on removal and adsorption of other economical metals from their different resources.

Compliance with ethical standards

Conflict of interest On behalf of all authors, the corresponding author states that there is no conflict of interest.

References

1. Zhou A, Wang J (2018) Recovery of U(VI) from simulated wastewater with thermally modified palygorskite beads. J Radioanal Nucl Chem 318:1119–1129
2. Donia AM, Atia AA, Moussa EMM, El-Sherif AM, Abd El-Magied MO (2009) Removal of uranium(VI) from aqueous solutions using glycidyl methacrylate chelating resins. Hydrometallurgy 95:183–189
3. Sadeek SA, El-Sayed MA, Amine MM, Abd El- Magied MO (2014) A chelating resin containing trihydroxybenzoic acid as the functional group; synthesis and adsorption behavior for Th(IV) and U(VI) ions. J Radioanal Nucl Chem 299:1299–1306
4. Sadeek SA, El-Sayed MA, Amine MM, El-Magied MOA (2014) Selective solid-phase extraction of U(VI) by amine functionalized glycidyl methacrylate. J Environ Chem Eng 2:293–303
5. Gładysz-Płaska A, Grabias E, Majdan M (2018) Simultaneous adsorption of uranium(VI) and phosphate on red clay. Prog Nucl Energy 104:150–159
6. Sun Z, Chen D, Chen B, Kong L, Su M (2018) Enhanced uranium(VI) adsorption by chitosan modified phosphate rock. Colloids Surf A 547:141–147
7. Liu Z, Liu D, Cai Z, Wang Y, Zhou L (2018) Synthesis of new type dipropyl imide chelating resin and its potential for uranium(VI) adsorption. J Radioanal Nucl Chem 318:1219–1227
8. Gado MA (2018) Sorption of thorium using magnetic graphene oxide polypyrrole composite synthesized from natural source. Sep Sci Technol 53:2016–2033
9. Abd El-Magied MO, Mansour A, Alsayed FA, Atrees MS, Abd Eldayem S (2018) Biosorption of beryllium from aqueous solutions onto modified chitosan resin: equilibrium, kinetic and thermodynamic study. J Dispersion Sci Technol 39:1597–1605
10. Abd El-Magied MO, Galhoum AA, Atia AA, Tolba AA, Maize MS, Vincent T, Guibal E (2017) Cellulose and chitosan derivatives for enhanced sorption of erbium(III). Colloids Surf A 529:580–593
11. Abd El-Magied MO (2016) Sorption of uranium ions from their aqueous solution by resins containing nanomagnetite particles. J Eng 2016:1–11
12. Sadeek SA, Moussa EM, El-Sayed MA, Amine MM, El-Magied MOA (2014) Uranium(VI) and thorium(IV) adsorption studies on chelating resin containing pentaethylenehexamine as a functional group. J Dispersion Sci Technol 35:926–933
13. Abd El-Magied MO, Dhmees AS, Abd El-Hamid AAM, Eldesouky EM (2018) Uranium extraction by sulfonated mesoporous silica derived from blast furnace slag. J Nucl Mater 509:295–304
14. Ang KL, Li D, Nikoloski AN (2017) The effectiveness of ion exchange resins in separating uranium and thorium from rare earth elements in acidic aqueous sulfate media. Part 1. Anionic and cationic resins. Hydrometallurgy 174:147–155
15. Ang KL, Li D, Nikoloski AN (2018) The effectiveness of ion exchange resins in separating uranium and thorium from rare earth elements in acidic aqueous sulfate media. Part 2. Chelating resins. Miner Eng 123:8–15
16. Hu W, Lu S, Song W, Chen T, Hayat T, Chen C, Liu H, Alsaedi NS (2018) Competitive adsorption of U(VI) and Co(II) on montmorillonite: a batch and spectroscopic approach. Appl Clay Sci 157:121–129
17. Klingenberg A, Seubert A (2002) Sulfoacylated poly(styrene–divinylbenzene) copolymers as resins for cation chromatography: comparison with sulfonated, dynamically coated and silica gel cation exchangers. J Chromatogr A 946:91–97
18. Malik MA (2009) Carbonyl groups in sulfonated styrene-divinylbenzene macroporous resins. Ind Eng Chem Res 48:696–6965

19. Pirogov AV, Chernova MV, Nemtseva DS, Shpigun OA (2003) Sulfonated and sulfoacylated poly(styrene–divinylbenzene) copolymers as packing materials for cation chromatography. Anal Bioanal Chem 376:745–752
20. El-Magied MOA, Mohammaden TF, El-Aassy IK, Gad HM, Hassan AM, Mahmoud MA (2017) Decontamination of uranium-polluted groundwater by chemically-enhanced, sawdust-activated carbon. Colloids Interf 1:1–17
21. Saluzzo C, Lamouille T, Herault D, Lemaire M (2002) Polymer-supported catalysts: enantioselective hydrogenation and hydrogen transfer reduction. Bioorg Med Chem Lett 12:1841–1844
22. Yu Y, Sun Y (1999) Macroporous poly(glycidyl methacrylate-triallyl isocyanurate-divinylbenzene) matrix as an anion-exchange resin for protein adsorption. J Chromatogr A 855:129–136
23. Marczenko Z (1986) Separation and Spectrophotometric determination of elements. Wiely, Toronto
24. Zahran MA, Mahmoud KF, Mahdy MA, Abd El-Hamid AM (2007) Leaching of gallium from Gattar granite, Eastern Desert, Egypt. Isot Radiat Res 39:115–126
25. Habashi F (1993) A textbook of hydrometallurgy. Department of Mining & Metallurgy, Laval University, Quebec City
26. Shalaby MH, Abu Zeid EK, Mahdy NM (2015) Erratum to: on the petrogenesis and evolution of U-rich granite: insights from mineral chemistry studies of Gattar granite, North Eastern Desert, Egypt. Arab J Geosci 8:3587
27. Hansink JD (1976) Equilibrium analyses of sandstone roll-front uranium deposits. Int Atomic Energy Ag Vienna 8:683–693
28. Stuckless JS, Nkomo IT, Wenner DB, Trump GV (1984) Geochemistry and uranium favourability of postorogenic granites of the north-eastern Arabian Shield, Kingdome of Saudi Arabia. Bull Fac Eart Sci King Abdel Aziz Univ 6:195–209
29. Shapiro L (1975) Rapid analysis of silicate, carbonate and phosphate rocks. US Geol Surv Bull 1401:70–76
30. Meinrath G (1981) Aquatic chemistry of uranium. Geoscience 1:1–100
31. Elshehy EA (2017) Removal of uranium ions from liquid radioactive waste using modified aluminosilica. Sep Sci Technol 52:1852–1861
32. Abd El-Magied MO, Hassan AM, Gad HMH, Mohammaden TF, Youssef MAM (2017) Removal of nickel (II) ions from aqueous solutions using modified activated carbon: a kinetic and equilibrium study. J Dispersion Sci Technol 39:862–873
33. Gado MA, Morsy A (2017) Preparation of poly-aniline–magnetic porous carbon composite for using as uranium adsorbent. Am J Mater Synth Process 2:32–40
34. Abd El-Magied MO, Elshehy EA, Manaa EA, Tolba AA, Atia AA (2016) Kinetics and thermodynamics studies on the recovery of thorium ions using amino resins with magnetic properties. Ind Eng Chem Res 55(2016):11338–11345
35. Abd El-Magied MO, Tolba AA, El-Gendy HS, Zaki SA, Ati AA (2017) Studies on the recovery of Th(IV) ions from nitric acid solutions using amino-magnetic glycidyl methacrylate resins and application to granite leach liquors. Hydrometallurgy 169:89–98
36. Elshehy EA, Shenashen MA, Abd El-Magied MO, El-Nahas AM, Tolan DA, Halada K, Atia AA, El-Safty SA (2017) Selective recovery of silver(I) ions from e-waste using cubically-multi-thiolated cage mesoporous monoliths. Eur J Inorg Chem 2017:4823–4833
37. Tag El-Din AF, Elshehy EA, Abd El-Magied MO, Atia AA, El-Khouly ME (2018) Decontamination of radioactive cesium ions using ordered mesoporous monetite. RSC Adv. 8:19041–19050
38. Abd El-Magied MO, Salem WM, Daher AA, Elshehy EA (2018) Fabrication of silica microspheres (HB/A@SI-MNS) for hafnium and zirconium recovery from zirconyl leach liquor. Colloids Interfaces 2:1–14
39. Mohamaden TF (1996) Correlative studies on some uraniferous radioactive granitic rocks in Qattar, El-Missikate, El-Erediya and Um-Ara area, Eastern desert, Egypt. M. Sc. In Geology, Ain Shams University, Egypt
40. Salman AB, Shalaby MH, Nosier LM (1990) Uranium province, northern RedSea Hills, Egypt. Int Earth Sci Congr 1:89–101